Measurement of the Sublayer Velocity Profile with Polymer Additive

Humberto Aquino* and Richard Lamontagne*
The Catholic University, Washington, D.C.

Several laser beam techniques measuring the velocity profile at the micro-interface between a polymer coated boundary flow and water were investigated. A method based on the Doppler effect of scattered light from trace particles in the fluid was first studied. The spatial resolution of this technique was found to be too poor for the present application. A second method based on the detection through a microscope of the scintillating light from trace particles was also investigated. The microscope was found to be adequate to provide the necessary spatial resolution (within 20μ); however, the light intensity of the scintillating patterns created by a low power laser beam was found to be too weak for detection by a photomultiplier tube. The technique finally adopted was simply to measure the mean elapsed time of illuminated trace particles traveling between two fixed slits placed at the image plane of the eyepiece of the microscope. The spatial resolution of this technique was further improved by focusing the illuminating laser beam to a small width of 20μ. The narrow beam was set parallel to and *centered* on the objective plane of the microscope. Flow profiles with a spatial resolution of 20μ have been achieved. Some turbulent flow profiles in a pipe are investigated. The existence of a slip layer is positively identified.

I. Introduction

TOMS phenomenon is a drag reduction by dilute polymer solutions in turbulent pipe flow. This phenomenon is thought by Savins (1964)[1] and Virk (1967)[2] to be divided into three separate regimes. The first regime, which is nearest to the wall, has no evident drag reduction because both polymer and solvent obey the same friction factor. The second regime, which is affected by the presence of polymer, does have a drag reduction. The friction factor for this zone is a function of all identifiable polymeric parameters such as the polymer molecular weight, concentration of the solution, temperature, and shear stress. The third regime can be identified as the normal turbulent layer which is controlled essentially by the eddy viscosity. The theory of these three regimes is presently deduced without proper measurement of the velocity field close to the wall since there was no known technique to measure the velocity field within the order of 200μ from the wall. Therefore, it is desirable to find a way to measure this field so that the nature of the three-layer hypothesis may be positively identified. The purpose of this paper is to present the development of such a technique.

In order to obtain an estimate of the thickness of the laminar sublayer, we may look at existing data for the turbulent boundary layer plotted in the normalized coordinates y^+ and U^+. The normalized distance from the wall y^+ is defined as

$$y^+ = yU^*/\nu \tag{1}$$

where y is the distance from the wall, ν is the kinematic viscosity and U^* is the shear velocity. The shear velocity is defined as

$$U^* = (\tau_0/\rho) \tag{2}$$

where τ_o is the shearing stress on the wall and ρ is the mass density of the fluid. The normalized velocity U^+ is defined as

$$U^+ = U/U^* \tag{3}$$

where U is the velocity of the fluid. In the normalized y^+ and U^+ coordinates, the phenomenon of drag reduction is expected to begin at approximately $y^+ = 4$. For water this is of the order of 100 μ; therefore, we need a measuring resolution of at least 50 μ.

To accomplish this goal we have considered three methods which are all based on laser light scattered from trace particles. They are the Doppler technique, the scintillating pattern technique, and the time delay technique. The first method is the standard Doppler technique, using a pair of coherent laser beams intersecting at the point of measurement. The velocity profile may be calculated through the variation of the Doppler frequency. This will be further discussed in Sec. IIA. In the second method, we tried to utilize the magnified scintillating pattern produced by reflecting coherent light from a trace particle to measure the velocity field. For this method, a photomultiplier tube and a microscope are used. Detailed discussion is presented in Sec. IIB. The third method is to employ two slits a known distance apart placed in the image plane of the eyepiece of the microscope. The time for each illuminated trace particle to traverse the distance between the two slits represents the speed of the particle. The spatial resolution of the distance from the wall is provided by the microscope. Using this technique, we were able to obtain detailed velocity profiles, in all three layers. Through the measured flow profiles the existence of a slip layer is identified. This technique will be described in detail in Sec. IIC.

II. Experimental Set Ups

A. Measuring Velocity Profile through the Doppler Effect

The standard Doppler technique is to employ a pair of coherent laser beams intersecting at the point of measurement. The wavelengths of the beams are modified by the fluid velocity, creating a Doppler effect which can be detected by a photomultiplier tube. This system is found to be inadequate for two reasons. One reason is that frequency of

Presented as Paper 73-39 at the AIAA 9th Annual Meeting and Technical Display, Washington D.C., January 8-10, 1973; submitted February 8, 1973; revision received September 16, 1974. The authors wish to acknowledge the helpful discussions and guidance of H. C. Ling, of the Department of Aerospace and Atmospheric Science, The Catholic University of America.

Index category: Boundary Layers and Convective Heat Transfer—Turbulent.

*Student, Department of Aerospace and Atmospheric Science. Student Member AIAA.

the Doppler effect is the same as the frequency created by scintillating patterns of the trace particles crossing the view of the detector. At present there is no practical means to filter out the scintillating frequency from the Doppler signal. Therefore, if one of the laser beams is obstructed, we still obtain the same signal as before. This shows that the signal from the scintillating patterns is stronger than that produced by the Doppler effect, which is commonly claimed to be observed. The other problem with this method is that the volume of the intersecting beams is too large for the proper spatial resolution required for the present work.

B. Measuring Velocity Profile by the Scintillating Pattern Technique

In this method we tried to utilize the scintillating pattern signal directly. Instead of using a simple lens to focus the point of the intersecting beams to the photomultiplier tube, we use a high-power microscope with a shallow focal depth. A single laser beam is placed parallel to the flow, and the optical axis of the microscope is placed perpendicular to both the beam and flow. Laser light reflected by a trace particle will produce a scintillating glow over the particles due to the interference of the coherent light. A photomicrograph of the scintillating particles is shown in Fig. 1. The average space between the dark spots should be equal to half the wavelength of the laser light which is approximately 1 μ. A photomultiplier tube with a small aperture is placed at the image plane of the eyepiece to obtain the signal of the moving scintillating pattern. The center frequency f_c of the signal can be related to the flow velocity U and light wavelength λ as

$$U=f_c\lambda/2 \qquad (4)$$

The reflected light from our 15 mw laser beam lacked the intensity needed for the photomultiplier to detect the signal. Although a more powerful laser beam may make this technique practical, because of heating and other technical problems it is not considered desirable for the present application.

C. Measuring Velocity by the Transit Time of a Trace Particle Crossing Two Slits

Instead of detecting the scintillating patterns of trace particles with a high gain microscope lens, we may detect the entire particle with a lower gain lens. With this the photomultiplier tube may pick up the whole particle as it traverses the plane of view. Two photomultiplier tubes are enclosed in separate black chambers with a small slit provided in each enclosure. These slits are 0.5 mm wide by 1.0 cm long and 2.5 cm apart. The slits are centered in the image plane of the eyepiece of the microscope. An illuminated particle traversing the object plane of the microscope will cross the slit of photomultiplier tube 1, and, after a delayed time, the slit of photomultiplier tube 2. The amplified signals from both photomultiplier tubes are connected to a dual beam oscilloscope with precision time base. The signal from photomultiplier tube 1 is used to trigger both beams of the oscilloscope. The time delay t of photomultiplier tube 2 may be read directly on the scope for each passage of a trace particle (see Fig. 2). The velocity of the particle is

$$U=S/t0_p \qquad (5)$$

where S is the spacing between the slits and 0_p is the optical gain of the microscope. Only signals with sharp spikes representing focused particles were accepted. All weak signals and wide pulses were eliminated. By using the mean value of a few hundred readings at each focused level from the wall, an accurate velocity profile can be plotted. For this technique, the spatial resolution was found to be limited by the focal depth of the microscope which is approximately 20 μ at an optical gain of 100.

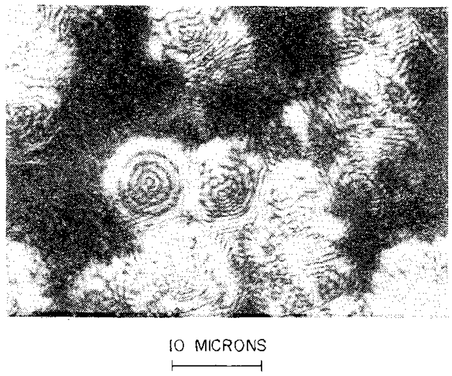

Fig. 1 Scintillating pattern.

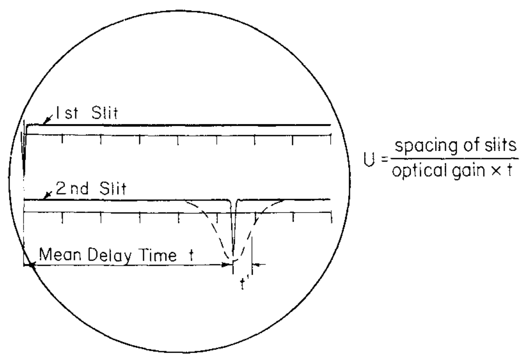

Fig. 2 Dual beam oscilloscope screen.

The whole test system consists of a water tank, pump, a 2-m long 1.27-cm diam Lucite tube, a manometer, a microscope, two photomultipliers, a polymer-injector, a laser light system, and an oscilloscope. This system is shown in Fig. 3. The water we used was stored in the tank for a few days before using to permit any entrapped air to escape. No extra trace particles were added to the water because enough already existed in the tap water. The water is pumped out of the tank through a calibrated flow meter for monitoring purposes. The pump is controlled with a Variac transformer and therefore the flow rate can also be controlled.

The concentrated polymer solution is efficiently distributed into the pipe system through a polymer injector. This is achieved by drilling small holes (0.06 cm diam) into the pipe around its circumference. An enclosure over these feed holes is connected to the reservoir of the concentrated polymer solution. The concentrated polymer is a solution of tap water and Polyox 301, with a ratio, of 10^3 to 1 by weight. The solution is gravity fed into the tube through a regulating valve and thus prevents the degradation of the polymer. Following the injector is the flow straightener. It consists of 5 plastic drinking straws, 4 cm long packed inside the pipe. No flow contraction is employed, so that turbulent flow is initiated at the entrance of the pipe. A minimum entrance length of 40 pipe diam is normally required to produce an established turbulent flow profile. In our experimental set up, an entrance length of 1 m or 77 pipe diam is provided. At the end of the entrance length there are 2 pressure taps spaced 61 cm apart. This is used for measuring the shear stress on the wall. The wall shear stress τ_o can be expressed in terms of the pressure gradient as

$$\tau_0=(\Delta p/\Delta x)\ (D/4) \qquad (6)$$

where Δp is the pressure drop between tap 1 and 2, Δx is the

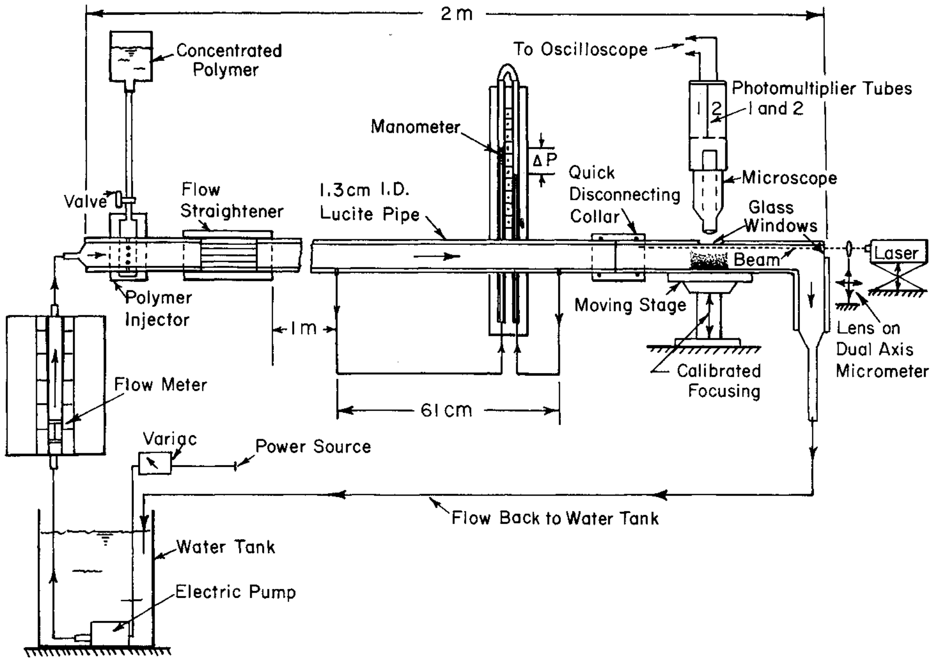

Fig. 3 Experimental set up.

distance between the two taps, and D is the inner diameter of the pipe. After the pressure taps is the microscope. The motion of the moving stage with respect to the objective of the microscope is calibrated in intervals of microns. The micrometer of the moving stage can be set to zero when the inner wall of the pipe is at the object plane of the microscope. Within the view of the microscope, the inside wall of the pipe is painted black to assure a black background. The top of the tube under the microscope is milled for mounting over a glass window which is 0.12 mm thick. The window is set flush with the inner wall of the pipe. It is important that this window be mounted with a high degree of precision with respect to both the pipe and the object plane of the microscope. After the microscope station, the pipe goes through a downward bend. At the top of the vertical bend, the pipe is again milled to provide a flat glass window for the laser beam (Fig. 3). The purpose of this window is to decrease defraction by having the laser beam enter perpendicular to it. The laser is mounted on an adjustable platform so that the beam can be properly directed into the flow system and aligned parallel to the pipe. A simple lens, supported on a mount with two micrometer axes is placed in between the laser and the glass window. With proper adjustments on the micrometers the beam can be precisely directed to the object plane of the microscope and also focused to a dimeter of 20 μ. This selective illumination of trace particles greatly enhances the spatial resolution of the optical system. The motion of the water, within a band of 20 μ and at a specified depth from the wall, is magnified by the microscope and detected by the two photomultipliers. An O-ring joint is provided a short distance upstream of the microscope for quick disconnection of the pipe system so that the glass windows may be cleaned from time to time.

III. Velocity Profiles and Drag Reduction

A. Turbulent Flow Profiles with Pure Water

The purpose of this experiment is to verify our mea surement technique against existing published data. Although there have been many studies on the turbulent boundary-layer theory, we chose the work of Townsend (1956).[3] The turbulent boundary-layer equation for water in the logarithmic regime is given by

$$U^+ = A \ln y^+ + B \tag{7}$$

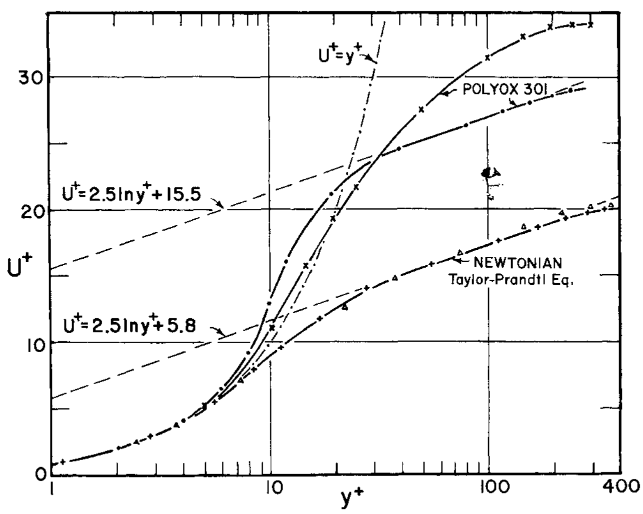

Fig. 4 Semi-log plot of velocity profiles.

where the coefficients A and B were found by Townsend to be 2.44 and 5.85, respectively. As can be seen in Fig. 4, the values we obtained with our present technique are $A = 2.5$ and $B = 5.8$. This confirms our profile for the logarithmic regime. We are able to continue to measure the profile all the way into the sublayer region which previously has not been measured accurately. The data shown in Fig. 4 also verify that the distribution of the laminar sublayer is governed by the functional relationship

$$U^+ = y^+ \tag{8}$$

This relationship is found to be valid to

$$U^+ < 5 \tag{9}$$

The intermediate region is found to be in the range

$$5 < y^+ < 40 \tag{10}$$

Above $y^+ = 40$ the curve begins to merge into the log profile of Eq. (7). The log profile is valid up to approximately y^+

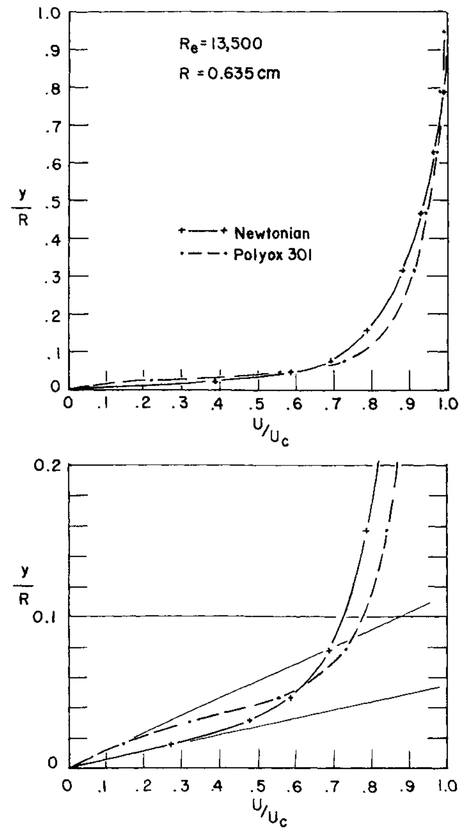

Fig. 5 Linear plot of velocity profiles. The distance y is normalized by the inner radius of the pipe R, and the velocity U normalized by the center line velocity U_c.

300, beyond which the eddy viscosity no longer increases linearly with y near the center of the pipe. The foregoing experimental data represent measurements taken at two Reynolds numbers of 13,500 and 20,300.

B. Turbulent Flow Profiles with Polyox 301 Additive

Two cases of flow with Polyox 301 additive were measured at Reynolds numbers corresponding to the cases with Newtonian fluid. The low Reynolds number case is plotted as the curve with solid circles shown in Fig. 4. We note that the data near the wall fall on the line of Eq. (8) which is the laminar sublayer for water. Because the log plot is normalized by the shearing stress at the wall, the relative shearing stress can be seen best on the linear plot of the profiles for both the cases of Newtonian and polymer solutions at the same Reynolds number of 13,500, as shown in Fig. 5. It is evident that the velocity gradient at the wall for the polymer case is half that for the case of pure water. Since we have shown that in the laminar sublayer the polymer solution has the same viscosity as pute water, the shearing stress at the wall must be approximately half that without polymer. In Fig. 4, at $4 < y^+ < 20$, the profile of the polymer case was found to be at the left of Eq. (8). The corresponding linear plot of this profile also can be seen in Fig. 5 as the curve between $0.02 < y/R < 0.05$, where R is the inner radius of the pipe and U_c is the center line velocity. We note that the velocity gradient at this zone is nearly twice that at the wall. Now, if the viscosity in this zone is the same or larger than that of water, then the shearing stress $\tau_0 = \mu(dU/dy)$ in this zone must be greater than that at the wall. s cannot be so because, in the absence of adverse local distribution of pressure gradient in a straight established flow, there is no possibility of an increase in shearing stress from that at the wall. For pipe flow the shearing stress distribution is expected to decrease with distance from the wall. Because the distance of this zone is very close to the wall, the shearing stress should be nearly the same as that at the wall; therefore, the only possibility is for the effective viscosity to be less than that of water. This zone may be identified as a slip zone.

For this case, with higher Reynolds number plotted as the line with x marks, again there is no slip in the laminar zone. For all cases, the actual distance y of the laminar zone is approximately less than 100 μ from the wall. We note that the slip layer for the higher flow case is thinner than the low speed case and falls closer to the left of the $y^+ = U^+$ line. The slipping action in this layer is again evident. Above the slip layer, both polymer cases have the regular turbulent log layer which is controlled essentially by the eddy viscosity, as evidenced by having the same coefficient A as the log equation. The higher flow case shows greater drag reduction than the lower flow case as indicated by the larger coefficient B. Therefore, drag reduction is dependent on the level of shearing stress. For the case when the slip profile is all on the right-hand side of $U^+ = y^+$, we will expect to have no drag reduction in the system.

IV. Conclusion

We have succeeded in developing a new technique for measuring a velocity field within 50 μ from the wall. By applying this technique, we have successfully mapped the detailed turbulent flow profile of a polymer water solution in a pipe. With this technique we have positively identified the nature of the slip layer produced by the polymer. However, the exact mechanics of this slipping action is still to be investigated with more thorough experimental measurements.

References

[1]Savins, J. G., "Drag Reduction Characteristics of Solutions of Macro Molecules in Turbulent Pipe Flow," *Society of Petroleum Engineers of the AIME Journal,* Vol. 4, 1964, pp. 203-215.

[2]Virk, P. S., Merrill, E. W., Mickley, H. S., Smith, K. A., and Mollo-Christensen, E. L., "The Toms Phenomenon: Turbulent Pipe Flow of Dilute Polymer Solutions," *Journal of Fluid Mechanics,* Vol. 30, Part 2, 1967, pp. 305-328.

[3]Townsend, A. A., "Turbulent Flow in Pipes and Channels," *The Structure of Turbulent Shear Flow,* Cambridge University Press, New York, 1956, pp. 194-223.